RSC Advances

ROYAL SOCIETY OF CHEMISTRY

www.rsc.org/advances

Journal Name

RSCPublishing

ARTICLE

Two novel structures based on an organic ligand with two different coordination modes

Cite this: DOI: 10.1039/x0xx00000x

Li-Na Xiao,[a,d] Xiao-Jing Song,[b] Li-Wei Fu,[a] Yang-Yang Hu,[a] Hai-Yang Guo,[a] Xiao-Bing Cui,*[a] Ming-Jun Jia,*[b] Xiao Zhang,*[c] Jia-Ning Xu,[a] Ji-Qing Xu[a]

Received 00th January 2012,
Accepted 00th January 2012

DOI: 10.1039/x0xx00000x

www.rsc.org/

Abstract two novel organic-inorganic hybrid compounds, namely $[Ag_6(bzmd)_2][SiW_{12}O_{40}]\cdot H_2O$ (**1**) and $[Ag_2(Hbzmd)_2][HPW_{12}O_{40}]$ (**2**) (Hbzmd=1-(p-(tetrazol-5-yl)benzyl)-2-(pyrid-2-yl)benzimidazole), have been synthesized and characterized by IR, UV, powder XRD, EDS, TG, cyclic voltammetry analysis, photoluminescent analysis, elemental analyses and single crystal X-ray diffraction. The two compounds represent two novel 3-D structures constructed from Keggin polyanions, metals and organic ligands. It should be noted that compound **1** is based on polyoxometalates, silvers and $bzmd^-$ ligands, whereas, compound 2 is based on polyoxometalates, silvers and Hbzmd ligands. The $bzmd^-$ ligand in compounds **1** and the Hbzmd ligand in **2** exhibit distinctly different coordination modes. Silvers and $bzmd^-$ ligands form a 3-D framework via Ag-N and Ag-π interactions in compound **1**, compound **1** also contains a pure inorganic 3-D framework, and then the two kinds of frameworks in compound **1** are fused into an unprecedented 3-D structure. Silvers and Hbzmd ligands form a 2-D framework via only Ag-N interactions in compound **2**, moreover, polyoxometalates in compound **2** are linked by silvers into a novel pure inorganic 2-D framework, and then two kinds of frameworks are further fused into a novel 3-D structure. In conclusion, two different 3-D frameworks and two different 2-D frameworks are respectively fused into two novel 3-D structures constructed from polyoxometalates, metals and organic ligands (POMMOFs).

Introduction

It has been widely recognized that polyoxometalates (POMs) exhibit a variety of structures and properties that make them useful in catalysis, material science and medicine.[1] POMs have also been found to be versatile inorganic building blocks for the construction of functional solid materials.[2] In the past few decades, with the advent of modern high-resolution and sophisticated instrumentation, the number of POM-based functional solid materials has been rising at an exponential rate.[3]

Recently, a new advance in POM chemistry is that a large number of compounds with 1-D, 2-D and 3-D structures constructed from the combination of POMs and transition metals or transition metal complexes (TMCs) have been obtained.[4-9] An intelligent choice of POMs and transition metals or TMCs may yield materials with fascinating structures and desirable properties. The diversity of POMs and transition metals or TMCs has led to a wide array of functional organic-inorganic hybrid materials. Up to now, most of POM species have already been applied to act as building blocks to be connected to transition metals or TMCs into extended structures, including Keggin, Dawson POMs and so on.

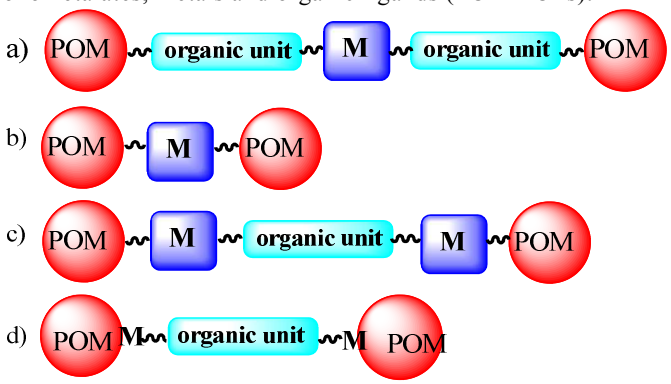

Scheme 1 Schematic representation of three major linking fashions of metals and POMs (a, b, c) and the linking fashion of POMOFs (d). M: transition metals.

Three main approaches have been developed for the linking of POMs and transition metals or TMCs. The first was represented by $[V_6O_{13}\{(OCH_2)_3C(NHCH_2C_6H_4CO_2)\}_2]^{4-}$, of which organic units connect POMs and metals into a novel framework (Scheme 1(a)).[4] The second uses dative bonds between POMs and transition metals or between POMs and TMC metals. A large number of such frameworks have been reported,[5-9] which were directed through interactions between transition metals or TMC metals serving as inorganic bridging linkers and oxygens of POMs (Scheme 1(b)). Recently a new approach has been developed for frameworks based on POMs and transition metals, of which, besides interactions between POMs and transition metals, a new kind of interactions can also occur via bidentate or multidentate organic ligands between or among transition metals. That is to say, both transition metals

and organic ligands in the frameworks act as bridges. Each transition metal acts as a bridge connecting a neighbouring POM and a neighbouring organic ligand, and simultaneously each organic ligand acts as a bridge connecting two neighbouring transition metals. Thus, through the two types of interactions, a kind of POM-based frameworks built from the connection of saturated POMs, metals and organic linkers, so-called POMMOFs, has emerged.[10] POMMOFs will exhibit a novel POM–M–L–M–POM linking fashion (Scheme 1(c)). The properties and diverse coordination modes of saturated POMs, metals together with the diversity of organic linkers provide an impetus for the synthesis of multifunctional materials.

There also exists a similar kind of POM based frameworks, so-called POMOFs.[11] We have found that most of POMOFs reported are based on substituted POMs (SPOMs) and organic ligands. The linking fashion of this kind of POM-based frameworks can be regarded as –SPOM–L–SPOM– (Scheme 1(d)), which is different with POMMOFs.

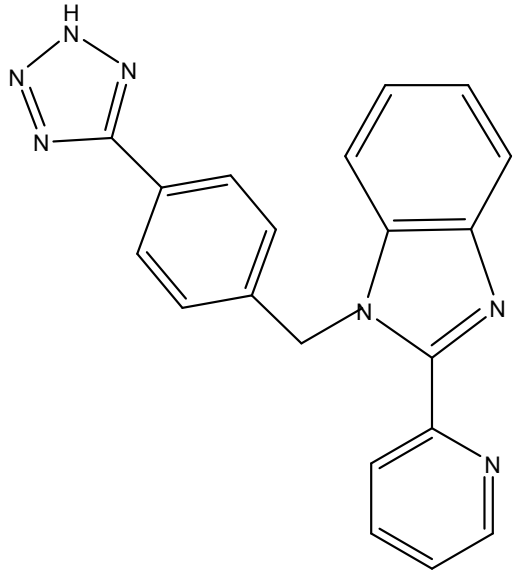

Scheme 2. Chemdraw structure of Hbzmd ligand.

We have synthesized several POMMOFs based on the popular traditional organic ligand 4,4-bpy. From then on, we began to search 3-D POMMOFs via using different organic ligands. Recently, we tried to use a multidentate organic ligand Hbzmd (Scheme 2), to prepare POMMOFs for this ligand is very large and can coordinate to metals via diverse and uncommon coordination modes. Notably, after a search of the CCDC structural database we found that still no complexes based on Hbzmd ligands have been reported up to now.

On the other hand, Ag(I), as a d^{10} transition metal, possesses high affinity for N and O donors, flexible coordination numbers of two to seven in covalent complexes, and versatile geometries, such as "linear", "seesaw", "square pyramidal", and "trigonal bipyramidal" coordination geometries, and so forth.[12] These features make Ag(I) often to be used as metallic linkers and good candidates in constructing metal organic frameworks. And recently, several research groups have devoted to this area of hybrids based on POMs and Ag(I) species and a large number of organic-inorganic materials based on Ag species and different POMs have been reported.[13-16]

According to the aforementioned points, we began to use Hbzmd ligands and silver ions to prepare novel 3-D POMMOFs, and fortunately, we successfully prepared two novel POMMOFs $[Ag_6(bzmd)_2][SiW_{12}O_{40}]\cdot H_2O$ (**1**) and $[Ag_2(Hbzmd)_2][HPW_{12}O_{40}]$ (**2**). In this manuscript, we report the syntheses and characterizations of the two. Single crystal analysis reveals that compound **1** contains the first novel 3-D metal organic framework formed via Ag-π and Ag-N interactions simultaneously, compound **1** also contains a novel 3-D pure inorganic framework structure, and then the two kinds of frameworks are fused by sharing silvers into a novel 3-D POMMOF structure. Compound **2** is also based on $bzmd^-$ ligands, and however, the structure of compound **2** is thoroughly different from that of compound **1**. Compound **2** contains a 2-D metal organic framework formed via only Ag-N interactions, and compound **2** also contains a novel 2-D pure inorganic framework, then the two kind 2-D frameworks are fused by sharing silvers into a novel 3-D POMMOF structure, too. In conclusion, two different 3-D frameworks and two different 2-D frameworks are respectively fused into two novel 3-D frameworks.

Experimental

Materials and methods

All chemicals used were of reagent grade and purchased commercially without further purification. C, H, N elemental analyses were carried out on a Perkin-Elmer 2400 CHN elemental analyser. Elemental analyses of Si, P, W, Mo and Cu were determined by inductively coupled plasma (ICP) analyses on a Perkin-Elmer Optima 3300DV ICP spectrometer. Infrared spectra were recorded as KBr pellets on a Perkin-Elmer SPECTRUM ONE FTIR spectrometer. Emission/excitation spectra were recorded on a RF-540 fluorescence spectrophotometer. UV-Vis spectra were recorded in dimethyl sulfoxide solution on a Shimadzu UV-3100 spectrophotometer. X-ray diffraction (XRD) patterns were obtained on a Siemens D5005 diffractometer using a Cu Kα radiation. Thermogravimetric (TG) curves were performed on a Perkin-Elmer TGA-7000 thermogravimetric analyzer in flowing N_2 with a temperature rate of $10^oC\cdot min^{-1}$. Electrochemical measurements were carried out on a CHI 660B electrochemical workstation. The working electrode was a glassy carbon, while the surface of the glassy carbon working electrode was polished with 1μm alumina and washed with distilled water before each experiment. The counter electrode was a Pt wire and an Ag/AgCl was served as reference electrode. The measurements were made at room temperature of 25℃.

Synthetic procedures

(a) **(b)**

Fig.1 crystal photos of compound **1** (a) and compound **2** (b).

Preparation of $[Ag_6(bzmd)_2][SiW_{12}O_{40}]\cdot H_2O$ (1) Compound **1** was synthesized hydrothermally from a mixture of $H_4[SiW_{12}O_{40}]\cdot xH_2O$ (FW≈2878.17, 0.5g, 0.174mmol), $C_6H_5NO_2$ (isonicotinic acid) (0.107g, 0.869mmol), $AgNO_3$ (0.101g, 0.595mmol), Hbzmd (0.05g, 0.142mmol) and distilled water (20ml). The pH of the mixture was necessarily adjusted

to 3 with $NH_3 \cdot H_2O$ solution. The mixture was heated under autogenous pressure at 160°C for 5 days and then left to cool to room temperature. Yellow block crystals (Fig.1(a)) could be isolated in about 37% yield (based on W). Anal. calcd for $C_{40}H_{30}Ag_6N_{14}O_{40}SiW_{12}$: Si 0.66, W 52.20, Ag 15.31, C 11.37, N 4.64, H 0.67%; Found: Si 0.61, W 51.86, Ag 15.27, C 11.11, N 4.60, H 0.65%. FT-IR (KBr, cm-1): 1619, 1595, 1470, 1446, 1423, 1341, 1303, 1257, 1137, 1113, 1012, 964, 921, 881, 787, 515, 384, 333.

Preparation of $[Ag_2(Hbzmd)_2][HPW_{12}O_{40}]$ (2) Compound **2** was synthesized hydrothermally from a mixture of $H_3[PW_{12}O_{40}] \cdot xH_2O$ (FW≈2880.05, 0.5g, 0.174mmol), $C_6H_5NO_2$ (isonicotinic acid) (0.12g, 0.975mmol), $AgNO_3$ (0.139g, 0.818mmol), Hbzmd (0.05g, 0.142mmol) and distilled water (20ml). The pH of the mixture was necessarily adjusted to 3 with $NH_3 \cdot H_2O$ solution. The mixture was heated under autogenous pressure at 160°C for 5 days and then left to cool to room temperature. Yellow block crystals (Fig.1(b)) could be isolated in about 31% yield (based on W). Anal. calcd for $C_{40}H_{31}Ag_2N_{14}O_{40}PW_{12}$: C 12.64, H 0.82, N 5.16; Found: C 11.83, H 0.50, N 4.65. FT-IR (KBr, cm-1): 1618, 1566, 1458, 1420, 1337, 1305, 1175, 1152, 1080, 970, 893, 812, 740, 508, 384, 333.

Crystallography

All data were collected on an Agilent Technology Super Nova Eos Dual system with a (Mo-K_α, λ = 0.71073Å for **1** and Cu-K_α, λ = 1.54184Å for **2**) microfocus source and focusing multilayer mirror optic. Data were collected under ambient conditions. Data collections, unit cell determinations and refinements, absorption corrections and data reductions were performed using the CrysAlisPro software from Agilent Technologies. The analytical absorption correction was performed by applying a face-based absorption correction as well as a spherical absorption correction. The crystals showed no evidence of crystal decay during the data collections. The structures were solved by direct methods and refined using full-matrix least squares on F^2 with the Wingx-2014.1 crystallographic software package. In the final refinements, all atoms were refined anisotropically in compounds **1** and **2**. In addition, the terminal five-member tetrazole ring of Hbzmd in compound **2** is disorderly distributed over two positions. It should be noted that such a disorder is ordinarily observed in crystallography. [17] Both the two crystallographically silver atoms in compound **2** are half-occupied. The TG curve of compound **2** is shown in Fig. s1. The sample weight continuously decreases with increasing temperature to 809ºC. The total weight loss was 17.6%, which is well consistent with the release of Hbzmd in compound **2** (calcd: 18.6%). We also do an EDS analysis of compound **2** which showed the presence of W, Ag and O in the crystals of compound **2** (Fig. s2). On the basis of TGA, EDS and CHN results, composition of compound **2** was found to be around $[Ag_2(Hbzmd)_2][HPW_{12}O_{40}]$. A summary of the crystallographic data and structure refinements for compounds **1** and **2** is given in Table **1**. CCDC number: 971294 for **1**, 993238 for **2**. These data can be obtained free of charge from The Cambridge Crystallographic Data Centre *via* www.ccdc.cam.ac.uk/data_request/cif.

Table 1. Crystal data and structure refinements for compounds **1** - **2**.

	Compound **1**	Compound **2**
Empirical formula	$C_{40}H_{30}Ag_6N_{14}O_{41}SiW_{12}$	$C_{40}H_{31}Ag_2N_{14}O_{40}PW_{12}$
Formula weight	4244.29	3800.7
Crystal system	Triclinic	Monoclinic
space group	P-1	p2(1)/n
a (Å)	12.376(3)	14.152(3)
b (Å)	15.058(3)	13.751(3)
c (Å)	18.787(4)	16.745(3)
α (°)	86.58(3)	90
β (°)	85.60(3)	93.81(3)
γ (°)	87.20(3)	90
Volume ($Å^3$)	3481.1(13)	3251.4(11)
Z	2	2
D_C ($Mg \cdot m^{-3}$)	4.049	3.882
μ (mm^{-1})	21.496	21.848
F(000)	3760	3372
θ for data collection	2.98 to 29.139	1.83 to 25.75
Reflections collected	30842	12870
Reflections unique	15928	6116
R(int)	0.0295	0.0236
Completeness to θ	99.8	99.9
parameters	1067	514
GOF on F^2	1.072	1.052
R^a [I>2σ(I)]	R_1 = 0.0569	0.0432
R^b (all data)	ωR_2 = 0.1135	ωR_2 = 0.1086

[a] $R_1 = \sum||F_0|-|F_c||/\sum|F_0|$. [b] $\omega R_2 = \{\sum [w (F_0^2-F_c^2)^2]/\sum[w(F_0^2)^2]\}^{1/2}$.

Results and discussion

Discussion the preparation procedures of compounds **1** and **2** are very similar to each other. The major difference of the two is the starting Keggin materials used. It is $H_4[SiW_{12}O_{40}] \cdot xH_2O$ for compound **1** but $H_3[PW_{12}O_{40}] \cdot xH_2O$ for compound **2**, and fortunately, both types of Keggin anions are successfully introduced into the final products.

The pH value of the reaction mixture for compound **1** is important for its preparation, attempts to synthesize compound **1** at pH values of 4 and 5 have been tried, but only unidentified amorphous materials were obtained.

The amounts of starting materials are important for the preparation of compound **1**. We have carried out the same procedure with only changed amounts of $AgNO_3$ or Hbzmd (see supporting information), and we only obtained some crystals unsuitable for crystal analysis or some unidentified amorphous materials. We also tried to synthesize analogue compounds at 180°C with the almost identical procedure with changed amounts of both $H_4[SiW_{12}O_{40}] \cdot xH_2O$ and isonicotinic acid (see supporting information), and also we only obtained some crystals unsuitable for crystal analysis.

The pH value of the reaction mixture for compound **2** is also important for its preparation, attempts to synthesize compound **2** at pH values of 2 and 4 have been tried, but only unidentified amorphous materials were obtained.

The effect of the amounts of starting materials for the preparation of compound **2** has also been studied. The same procedure with only changed amounts of $H_3[PW_{12}O_{40}] \cdot xH_2O$ has been carried out (see supporting information), and we only obtained some crystals unsuitable for crystal analysis. The same procedure with both changed amounts of isonicotinic acid and Hbzmd and with both changed amounts of $H_3[PW_{12}O_{40}] \cdot xH_2O$ and isonicotinic acid have also been done (see supporting information), but we only obtained some unidentified amorphous materials. Based on above-mentioned experiments, we found that the current procedures for compounds **1** and **2** are both the optimal ones. Little changes of temperature, pH, and amounts of starting materials of the synthesis procedures will not yield compounds **1** and **2**.

We also tried to synthesize analogue compounds of compound **2** using the same procedure with different carboxylate acids (oxalic acid (0.167g, 1.85mmol) or 1,3-benzenedicarboxylic acid (0.133g, 0.801mmol)) taking the place of isonicotinic acid (0.12g, 0.975mmol), and we also only obtained some unidentified amorphous materials.

In both procedures, isonicotinic acids were used as a starting material, which are not incorporated in both final products. The role of isonicotinic acids is still elusive.

Perhaps the different starting materials are the main reason for the formations of the two novel compounds. Compound **1** is based on the anion $[SiW_{12}O_{40}]^{4-}$ which contains four negative charge, whereas the anion in compound **2** is $[HPW_{12}O_{40}]^{2-}$ with three negative charge. Therefore, there are six and four silvers in chemical formulas of compounds **1** and **2**. It is well known the two Keggin ions in compounds **1** and **2** have almost identical shape and size but different negative charge, and the two thus must be accompanied with different number of silvers. Therefore, silver coordination units of compounds **1** and **2** must be different, the silver coordination units of compound **1** should be tighter, and the silver coordination units of compound **2** should be relatively looser.

Structure of compound 1 Single crystal X-ray analysis reveals that the POM of compound **1** is $[SiW_{12}O_{40}]^{4-}$. Bond valence sums (BVS) for W atoms in compound **1** were calculated using the parameters given by Brown (Table s1).[18] Results indicate that the twelve tungstens are in the +6 oxidation state. The asymmetric unit of compound **1** is constructed from two halves of POMs $[SiW_{12}O_{40}]^{4-}$, six silvers and two bzmd$^-$. The two bzmd$^-$ ligands present two different coordination modes. As shown in Fig. 2(a), N(1) bzmd$^-$ links one Ag(1), one Ag(2), one Ag(5), one Ag(6) and two Ag(3) via Ag-N dative bonds. N(1) and N(4) respectively coordinates to only Ag(1) and Ag(3), N(3) coordinates to both Ag(5a) and Ag(6a) simultaneously. Both N(6) and N(7) with Ag(3b, a: 3-x, -2-y, 4-z) form a stable five-membered chelate ring.

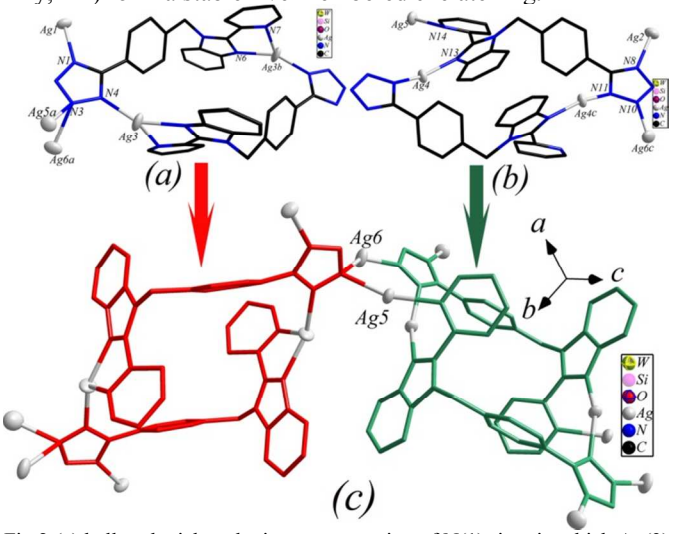

Fig.2 (a) ball-and-stick and wire representation of N(1) ring, in which Ag(3) adopts a trigonal pyramidal geometry; (b) ball-and-stick and wire representation of N(8) ring, in which Ag(4) has a linear geometry; (c) 1-D chain structure viewing along the (1, 1, 1) direction formed by N(1) and N(8) rings linked by Ag(5) and Ag(6) via Ag-N bonds. N(1) ring in (c) is in red, and N(8) ring in (c) is in green. Hydrogen atoms were omitted for clarity. Symmetry code: a (1+x, y, z), b (3-x, -2-y, 4-z), c (2-x, -1-y, 3-z).

As shown in Fig. 2(b), N(8), N(10), N(11), N(13) and N(14) of N(8) bzmd$^-$ are bound to only Ag(2), Ag(6d), Ag(4d), Ag(4) and Ag(5), respectively. It should be noted that Ag-N distances between nitrogen atoms of N(1) or N(8) bzmd$^-$ and their neighboring silver ions are comparable and in the range of 2.11(1)-2.45(1)Å.

Each N(1) bzmd$^-$ coordinates to two Ag(3) via both monodentate and bidentate modes, which implies that N(1) bzmd$^-$ acts a μ_2-bridge joins two Ag(3). On the other hand, each Ag(3) joins two N(1) bzmd$^-$. Therefore, a novel ring (N(1) ring) consisting of two N(1) bzmd$^-$ and two Ag(3) is formed, as shown in Fig. 2(a). It should be noted that the oval ring is approximately 11.60×8.38Å.

Each N(8) bzmd$^-$ coordinates to two Ag(4) via a bis-monodentate coordination mode and each Ag(4) is coordinated by two N(8) bzmd$^-$. Thus, a similar ring (N(8) ring) being composed of two N(8) bzmd$^-$ and two Ag(4) comes into being with an oval ring approximately 10.81×8.75Å. N(1) bzmd$^-$ and N(8) bzmd$^-$ rings are linked by Ag(5) and Ag(6) as two bridges into a novel 1-D Ag-N chain running along the (1, 1, -1) direction, as shown in Fig. 2(c). It should be noted that N(1) and N(8) rings in the chain are arranged alternately.

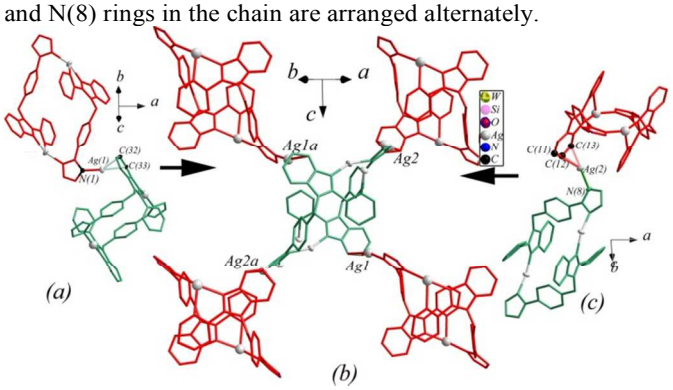

Fig. 3 (a) binding modes of Ag(1) and its neighboring phenol ring; (c) binding mode of Ag(2) and its neighboring ring; (b) 2-D layer structure viewing along the (1, 1, 0) direction formed by N(1) and N(8) rings linked by Ag(1) and Ag(2) via Ag-C interaction. N(1) ring is in red, and N(8) ring is in green. Hydrogen atoms were omitted for clarity. Symmetry code: a (2-x, -1-y, 3-z).

N(1) and N(8) rings are also further linked to each other by Ag(2) into another different novel chain. Each Ag(2) is bonded to not only N(8) from N(8) ring but also three carbons of the phenol from N(1) ring. The binding mode of Ag(2) is displayed in Fig. 3(c), Ag(2) lies almost directly above C(12) of the phenyl ring with bond angles Ag(2)-C(12)-C(11), 88(1)° and Ag(2)-C(12)-C(13), 92(1)° and distances Ag(2)-C(11) 2.68(2), Ag(2)-C(12) 2.34(2) and Ag(2)-C(13) 2.7473(6)Å. Since these Ag-C distances are below the upper limit of 2.92Å for effective π interaction between silver (I) and aryl carbon, the coordination mode can be regarded as η_3.[19] Two precedents exhibiting weaker η_3-π interactions have been found in $[(PhCH_2NMe_3)Ag_7(C_2)(CF_3CO_2)_6]_n$[19] and $[Ag(GaCl_4)\cdot\{(p\text{-}C_6H_4CH_2CH_2)_2\}]$.[20] Therefore, N(8) and N(1) rings are linked by Ag(2) via Ag(2)-π interactions into a novel 1-D Ag-π chain running along the (-1, 1, 1) direction with N(8) and N(1) rings arranged alternately (Fig. 3).

Except Ag(2)-π interactions, there also exist another different kind of Ag-π interactions between N(1) and N(8) rings. Ag(1) is coordinated by not only N(2) from N(1) ring but also two carbons of the phenol from N(8) ring. The binding mode of Ag(1) is shown in Fig. 3(a). Ag(1) is also almost directly above C(32) and C(33) of the phenol ring with bond angles Ag(1)-C(32)-C(33), 82(1)° and Ag(1)-C(33)-C(32), 66.2(9)° and distances Ag(1)-C(32) 2.38(2) and Ag(1)-C(33) 2.58(2)Å. The coordination mode can be regarded as η_2. Two precedents exhibiting weaker η_2-π interactions have been found in $(C_6H_{11}C_6H_5)_2AgClO_4$[21] and $[Ag_9$(5-phenyl-1H-

tetrazole)$_5$][$PMo_{12}O_{40}$]·H_2O.[22] Ag(1)-π interactions are very important for the arrangement of N(1) and N(8) rings. N(1) and N(8) rings are linked by Ag(1) via Ag(1)-π interactions into a novel 1-D Ag-π chain running along the (1, -1, 1) direction with N(1) and N(8) rings arranged alternately. It should be noted that the Ag-π chain formed via Ag(1)-π interactions is perpendicular to the Ag-π chain formed via Ag(2)-π interactions, as shown in Fig. 3(b).

Therefore, two different Ag-π chains are interwoven into a novel 2-D layer structure, as shown in Fig. 3(b). That is to say, each N(8) ring is linked to four neighboring N(1) rings and each N(1) ring is linked to four neighboring N(8) rings via Ag-π interactions into a novel 2-D layer structure with large channels running along the (1, 1, 0) direction (as shown in Fig. 3(b)). The size of the channel is about 14.19×13.26Å.

Ag-π bonds in compound **1** are thoroughly different from those previously reported ones, which play the most important role in the formation of the packing structure of compound **1**. Ag-π bonds link neighboring 1-D Ag-N chains into a novel 3-D framework structure with channels running along the (1, 1, -1) direction, where the channel size is about 14.19×13.26Å, as shown in Fig. 4. To the best of our knowledge, it is the first 3-D framework structure formed via both Ag-π and Ag-N interactions. There are also channels running through the structure viewing along the (1, 0, 0), (0, 1, 0) and (0, 0, 1) direction. Along the (1, 0, 0) and (0, 1, 0) directions, parallelogram channels were observed, each of which is formed by two N(1) and two N(8) rings with size of 7.83×12.65Å.

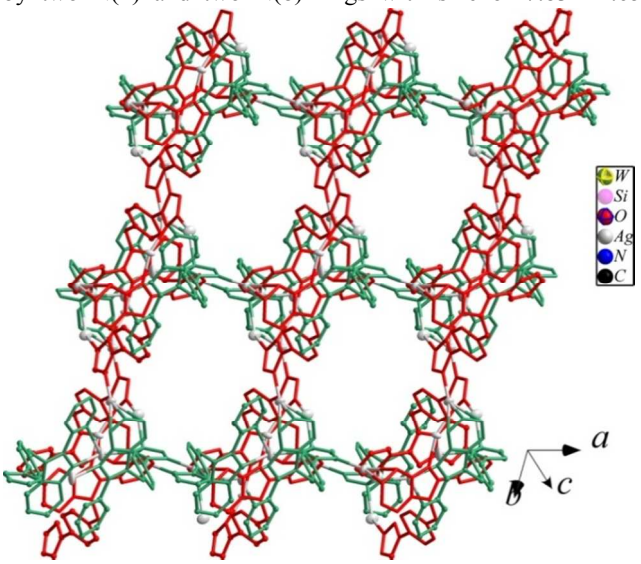

Three kinds of channels were observed when viewed along the (0, 0, 1) direction, one is a "+" shaped channel, and the other two are just the N(1) and N(8) rings running along the (0, 0, 1) direction.

Fig. 4 3-D framework formed via Ag-N and Ag-C interactions viewing along the (1, 1, -1) direction. N(1) $bzmd^-$ is in red, and N(8) $bzmd^-$ is in green. Hydrogen atoms were omitted for clarity.

Coordination polymers are a kind of molecular materials which have infinite metal-ligand backbones connected by coordination bonds. Ligands are generally bound to the central metal atom by a coordinate covalent bond. Organic ligands used in the construction of coordination polymers can be mainly divided into two different classes: nitrogen-containing organic ones and oxygen-containing organic ones or carboxylates. It should be noted that the pyridine carboxylates can be regarded as members of carboxylates. Accordingly, the coordinate covalent bonds can be mainly grouped into two types: metal-N bonds and metal-O bonds. Except for the two types of organic ligands, there are also organic ligands such as alkenes whose π bonds can coordinate to empty metal orbitals. An example is ethene in the complex known as Zeiss's salt, $K[PtCl_3(C_2H_4)]·H_2O$. And accordingly, the coordinate covalent bond can be metal-π bond. It is now clear that these metal-π interactions provide a powerful tool for the building of novel molecular architectures and allow the introduction of a wide variety of useful electric and electrochemical properties.[23]

Most of MOFs or coordination polymers are based on different nitrogen-containing and carboxylate ligands. The diversity of nitrogen-containing and carboxylate ligands give rise to a large number of MOFs with interesting structures and properties. However, organic ligands whose π bonds can coordinate to empty metal orbitals are rarely used in the construction of MOFs, to the best of our knowledge, MOFs based on metal-π bonds are very rarely reported previously.[23b]

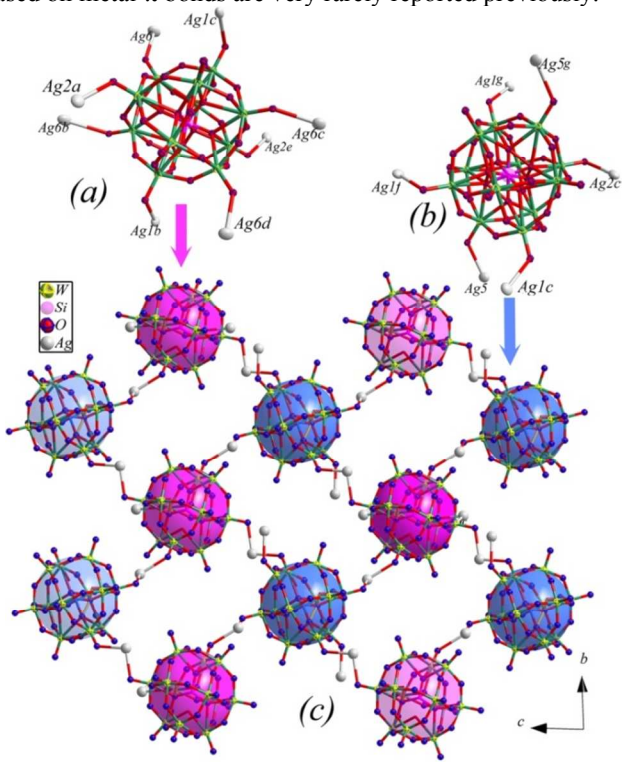

Fig. 5. (a) Coordination mode of Si(1) POM; (b) coordination mode of Si(2) POM; (c) 3-D pure inorganic framework formed by POMs and silver ions. The pink ball represents the Si(1) POM and the blue ball represents the Si(2) POM. Hydrogen, carbon and nitrogen atoms were omitted for clarity. Symmetry code: a (-1+x, y, 1+z), b (1-x, -1-y, 4-z), c (-1+x, y, z), d (-x, -1-y, 4-z), e (1-x, -1-y, 3-z), f (2-x, -2-y, 3-z), g (1-x, -2-y, 3-z).

The most unusual feature of compound **1** is that it contains Keggin polyanions which exhibit covalent interactions with the framework formed via Ag-π and Ag-N interactions. It should be noted that there are two different types of Keggin anions with Si(1) and Si(2) as heteroatoms. As shown in Fig. 5, Si(1) POM acting as a multi-dentate ligand coordinates to eight silvers, four of which (Ag(6)) serve as two double-bridges, the other four of which (Ag(1) and Ag(2)) act as four inorganic bridges linking $[SiW_{12}O_{40}]^{4-}$. On the other hand, Si(2) POM is bound to six silvers (Fig. 5), four of which (Ag(1) and Ag(2)) behave as four bridges linking $[SiW_{12}O_{40}]^{4-}$, but the other two of which (Ag(5)) are only supported by $[SiW_{12}O_{40}]^{4-}$. Ag(1) displays an irregular polyhedral geometry with a $N_1C_2O_2$ donor set, in which the two carbons and the nitrogen are from two $bzmd^-$ and the two oxygens are from two $[SiW_{12}O_{40}]^{4-}$. Ag(2) exhibits

another irregular polyhedral geometry with a $N_1C_3O_2$ donor set, in which the three carbons and the nitrogen are from two bzmd$^-$ and the two oxygens are from two $[SiW_{12}O_{40}]^{4-}$. Ag(6) presents a trigonal bipyramidal geometry with a $N_2O_2(H_2O)_1$ donor set, including one coordinated water molecule, two nitrogens from two bzmd$^-$ and the two oxygens are from two $[SiW_{12}O_{40}]^{4-}$. The geometry around Ag(5) is a trigonal pyramid which is defined by two nitrogens from two bzmd$^-$ and one oxygen from $[SiW_{12}O_{40}]^{4-}$. Ag-O distances are in the range of 2.38(1)-2.8614(9)Å. In one word, Si(1) and Si(2) POMs are connected to each other by silvers into a novel 3-D pure inorganic framework structure with parallelogram-shaped channels running along the *a* axis (Fig. 5). The size of the channel is about 16.35×10.97Å.

As mentioned above, Ag(1) and Ag(2) are not only very important for the formation of the metal-organic framework via Ag-π and Ag-N interactions, also are very important for the formation of the pure inorganic 3-D framework. That is to say, Ag(1) and Ag(2) are shared by the two kinds of 3-D frameworks. Therefore, the structure of compound **1** is a novel 3-D POMMOF structure fused by the metal metal-organic framework via Ag-π and Ag-N interactions and the pure inorganic 3-D frameworks (Fig. s3).

Though compounds based on η_3-π and η_2-π interactions have been reported before, compounds containing both of the two are very rare. To the best of our knowledge, only one compound which is based on novel 2-D networks linked by 5-phenyl-1H-tetrazole ligands and Ag ions through both η_2-π and η_3-π interactions has been reported very recently by Kong and Ren et al.[24] However, compound **1** is thoroughly different from that of Kong and Ren's compound. Firstly, compound **1** is based on bzmd$^-$ ligands and Kong and Ren's one is based on 5-phenyl-1H-tetrazole ligands. Notably, the two ligands are thoroughly different, though both of which contains phenol rings and aromatic tetrazole rings. Secondly, compound **1** and Kong and Ren's one are formed by different POMs, our compound is based on the well-known Keggin one, and Kong and Ren's case is based on P_5W_{30} clusters. Finally, and most importantly, our compound is based on a 3-D framework structure though both η_3-π and η_2-π interactions, while Kong and Ren's case is based on a 2-D layer structure though both η_3-π and η_2-π interactions.

Structure of compound 2 Crystal analysis reveals that the asymmetric unit of compound **2** is constructed from half a $[HPW_{12}O_{40}]^{2-}$ ion, two half-occupied silvers and a protonated Hbzmd ligand. Bond valence sum calculations reveal that the formula of the anion should be $[HPW_{12}O_{40}]^{2-}$ (Table s2).[18] The two crystallographically independent silver ions are both half-occupied, which means that all the silver ions in compound **2** are disorderedly distributed.

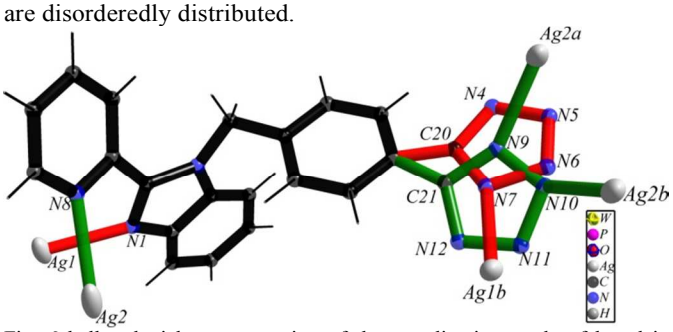

Fig. 6 ball-and-stick representation of the coordination mode of bzmd in compound **2**. Symmetry code: a (0.5-x, -0.5+y, 0.5-z), b (0.5+x, 2.5-y, -0.5+z).

Hbzmd in compound **2** adopts a thoroughly different coordination mode from bzmd$^-$ in compound **1**. As shown in Fig. 6, Hbzmd acting as a μ_5-bridge linking two Ag(1) and three Ag(2) via its different nitrogens. N(1) and N(8) respectively coordinate to only Ag(1) and Ag(2) with Ag-N distances of 2.345(7)-2.493(9)Å. Actually, since the five-member tetrazole ring of Hbzmd is disorderly distributed over two sites, combined with disorderly distributed silver ions around it, the coordination mode of the tetrazole ring is very complex. As shown in Fig. 6, each atom of the tetrazole ring is split into two with an occupancy factor of 0.5, indicating that a pair of equivalent disordered tetrazole rings each comprising a set of five halves of atoms are observed. The two equivalent disordered tetrazole rings and the disordered silver ions around the two can be grouped into two disordered parts (see the cif file of compound **2**): Ag(2), C(21) and N(9) to N(12) belong to PART 1, Ag(1), C(20) and N(4) to N(7) belong to PART 2, those belonging to either PART 1 or PART 2 are never present at any one time. Therefore, Ag-N distances between each tetrazole ring and its neighboring disordered silver ions in each part are in the range of 2.2(1)-2.30(9)Å.

Ag(2) is coordinated by N(9), N(10) and N(8) from three Hbzmd, and Ag(2), N(9) and N(10) belong to two disordered PART 1 groups, whereas N(8) is ordered. Ag(1) is bound to N(7) and N(1) from two Hbzmd, and Ag(1) and N(7) belong to a disordered PART 2 group, whereas N(1) is ordered. It should be noted that those linkages belonging to either PART 1 or PART 2 are never present at any one time. Hbzmd and disordered Ag(2) in compound **2** form a novel 2-D layer structure as shown in Fig. 7(a). The 2-D packing structure is very interesting, it contains S-shaped and reverse S-shaped channels both running along the (1, 0, 1) direction, moreover, S-shaped and reverse S-shaped channels are packed tightly as shown in Fig. 7(b). Hbzmd and disordered Ag(1) in compound **2** form a 1-D chain structure running along the (1, 0, -1) direction, and then the 1-D chains are arranged in a parallel manner along the *b* axis into a 2-D supramolecular layer structure, as shown in Fig. 7(c). Therefore, the actual packing structure formed by Hbzmd ligands and disordered Ag ions in compound **2** is a 2-D layer one. Because all the Ag positions are half-occupied or disorderedly distributed, the shapes of actual channels should be more complex and diverse which can be formed by two or more S-shaped or reverse S-shaped ones merging into one via deleting linking PART 2 atoms.

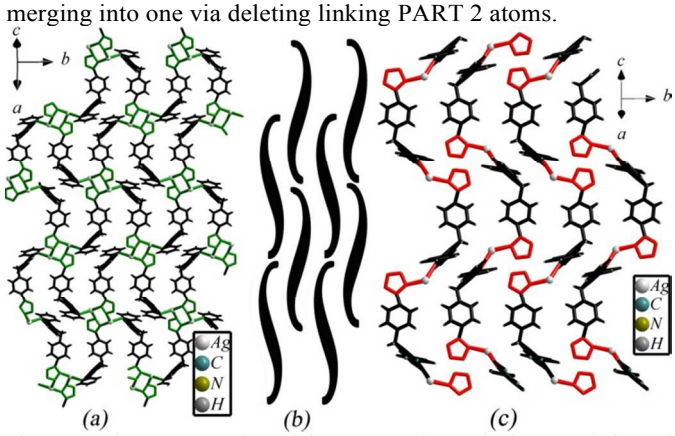

Fig. 7 (a) wire representation of the 2-D metal-organic framework formed by Hbzmd ligands and disordered Ag(2) ions, disordered part 2 atoms are in green. (b) Schematic representation of S-shaped and reverse S-shaped channels in the 2-D framework. (c) Wire representation of the 1-D metal-organic chain formed by Hbzmd ligands and disordered Ag(1) ions, disordered part 1 atoms are in red.

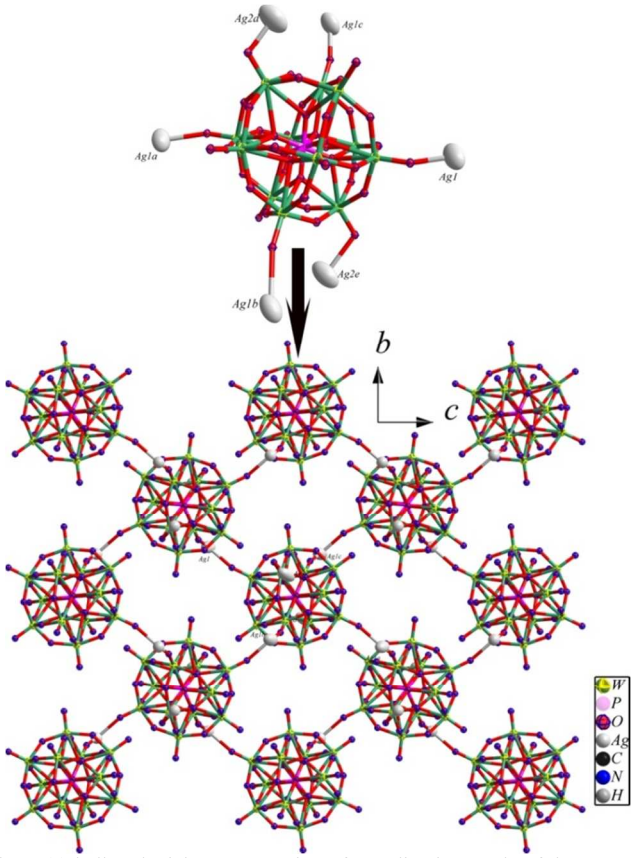

Fig. 8 (a) ball-and-stick representation of coordination mode of the POM in compound 2; and (b) ball-and-stick representation of the 2-D pure inorganic framework in compound **2**. Hydrogen, carbon and nitrogen atoms were omitted for clarity.

Another unusual feature of compound **2** is that POMs and silver ions also form an extended pure inorganic framework structure just like those in compound **1**. In contrast to the 3-D framework in compound **1**, it is a novel 2-D framework in compound **2**. As shown in Fig. 8, each POM acting as a hexadentate ligand coordinates to four Ag(1) and two Ag(2) ions. It should be noted that the roles of Ag(1) and Ag(2) ions are very different from each other. Ag(1) serves as an inorganic bridge linking two POMs, whereas Ag(2) is only supported by a POM. Ag-O distances are in the range of 2.38(1)-2.47(1)Å. It should be noted that all the sites of Ag(1) atoms of the inorganic 2-D framework are half-occupied.

Ag(1) and Ag(2) are not only very important for the formation of the 2-D metal-organic framework, also are very important for the formation of the pure inorganic 2-D framework. That is to say, Ag(1) and Ag(2) are shared by the two kinds of 2-D frameworks. Therefore, a novel 3-D POMMOF structure fused by the 2-D metal-organic framework and the 2-D pure inorganic framework come into being (Fig. s4).

Looking at the geometry and intermolecular environment (potential H-bonding) of the tungstate cage in compound **2**, there is no obvious site where a proton can be attached. Further analysis reveals that there is a short intermolecular contact N(8)···N(5a)(a: 0.5-x, 0.5+y, 0.5-z) of 2.7840(6)Å, which can well be a strong hydrogen bond. The strong hydrogen bond demonstrated that the added organic ligand as a starting material for the preparation of compound **2** is not deprotonated in the final product (scheme 2). The existence of the hydrogen bond further demonstrated that the formula of compound **2** should be $[Ag_2(Hbzmd)_2][HPW_{12}O_{40}]$.

Characterization

IR spectrum The IR spectrum of compound **1** was detailedly described as below as an example. The IR spectrum of compound **1** is shown in Fig. s5, in the spectrum, the characteristic band at 964cm^{-1} is attributed to υ(W-O$_t$), the band at 881 cm^{-1} is ascribed to υ(W-O$_b$-W), and the band at 787cm^{-1} is due to υ(W-O$_c$). The stretching of Si-O bonds is observed at the spectrum band of 921cm^{-1}. The IR spectrum of compound **2** is similar to that of compound **1**, which exhibits characteristic bands at 970, 893, 812cm^{-1} for **2** ascribed to υ(W-O$_t$), υ(W-O$_b$-W) and υ(W-O$_c$), respectively, stretching of P-O bonds is observed at the spectrum band of 1080cm^{-1}. In addition, the absorption bands at 1619-1113cm^{-1} are due to vibrations of bzmd$^-$ ligands in both compounds **1** and **2**.

XRD analysis The X-ray powder diffraction patterns of compounds **1** and **2** are in good agreement with the simulated XRD patterns, confirming the phase purity of the two compounds (Fig. s6). The differences in reflection intensities are probably due to preferential orientations in the powder samples of compounds **1** and **2**.

UV spectrum The UV spectra of compounds **1** and **2,** in the range of 220-400 nm, are presented in Fig. s7. The UV spectrum of compound **1** displays an intense broad absorption peak centered about 260nm assigned to O→W charge transfer and an obvious shoulder peak centered at about 307nm ascribed to n→π^* transitions of bzmd$^-$ ligands in compound **1**. The UV spectrum of compound **2** is similar to that of compound **1**, which also shows a peak centered about 260nm and a shoulder peak centered at about 307nm assigned to O→W charge transfer and n→π^* transitions of bzmd$^-$ ligands in compound **2**.

XPS analysis The tungsten oxidation state calculated from bond valence sum calculations was confirmed by the XPS spectrum for **1** (Fig. s8), which gives a W 4f$_{5/2}$ line at 37.4eV and a W 4f$_{7/2}$ line at 35.6eV and a ΔE of 1.9eV attributed to W^{6+} in compound **1**.

The oxidation states for tungsten atoms of **2** are further confirmed by the XPS analysis too. The XPS spectrum for **2** presents similar W4f$_{7/2}$ and W4f$_{5/2}$ lines to those of compound **1** at 34.6eV and 36.7eV and a ΔE of 2.1eV ascribed to W^{6+} (as shown in Fig. s8) in compound **2**.

Cyclic voltammogram The cyclic voltammogram of the DMSO solution of compound **1** in the mixture of 1 mol/L H_2SO_4 and 0.5mol/L $NaSO_4$ solutions at the scan rate of 100mV·s^{-1} is presented in the potential range of 0 to -800 mV (Fig. s9). There exist three reversible redox peaks and with the mean peak potentials ($E_{1/2}$=(E_{pa}+E_{pc})/2) at -583, -445 and -278mV for compound **1**. The three redox peaks correspond to one two-electron and two consecutive one-electron processes of W in compound **1**.[25] The cyclic voltammogram of compound **2** is very similar to that of compound **1**, which also shows three reversible redox peaks with the mean peak potentials ($E_{1/2}$=(E_{pa}+E_{pc})/2) at -608, -336 and -34mV, and these peaks should also be ascribed to one two-electron and two consecutive one-electron processes of W in compound **2**.[25]

Photoluminescence property The solid state photoluminescence properties of compounds **1** and **2** were studied. The emission spectrum of compounds **1** and **2** at room temperature is depicted in Fig. s10. It can be observed that an intense emission occurs at 425 nm (λex = 372 nm) for compound **1** and 423 nm (λex = 372 nm) for compound **2**, which can be assigned to the emission of intra-ligand charge

transfer. The emission peak in compounds **1** and **2** is blue shifted relative to that of the free bzmd⁻ ligand (λmax = 451nm). The blue shift has been regarded as due to the complexation of the organic ligand with silver atoms.

photocatalytic property In a typical process, 1.18μmol compound **1** (5mg) or **2** (4.7mg) were dissolved in 100 mL rhodamine B (RhB) solutions (1.0×10^{-5}mol·L^{-1}), respectively, the solution was agitated in an ultrasonic bath for 20min in the dark and then magnetically stirred in the dark for about 30min. The solution was finally exposed to UV irradiation from a 300W Hg lamp at a distance of about 4-5 cm between the liquid surface and the lamp. The solution was stirred during irradiation. At 30min intervals, 5mL of samples were taken out from the beaker, and subsequently analyzed by UV-visible spectroscopy (Fig. 9). The photodegradation process of RhB without any photocatalyst has been studied for comparison, and only 10.2% of RhB was photodegraded after 3h. Changes in C_t/C_0 plot of RhB solutions versus reaction time were shown in Fig. 9. Compared with RhB without any photocatalyst, the absorption peaks of compounds **1**–**2** decreased obviously upon irradiation, indicating that these compounds have excellent photocatalysis properties. It also reveals that compounds **1-2** are outstanding photocatalysts for photocatalytic degradation of RhB.

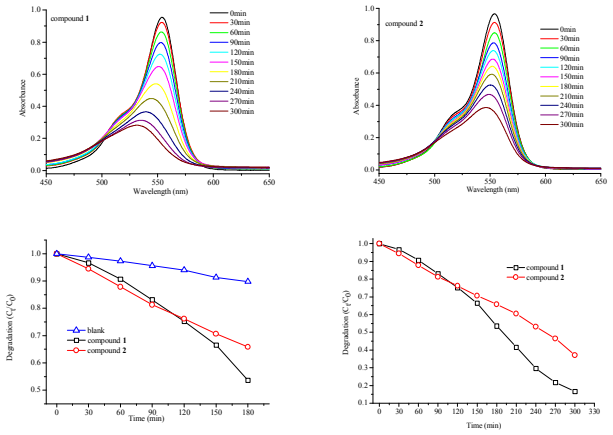

Fig. 9. (a) Absorption spectra of the RhB solution during the decomposition reaction under UV irradiation in the presence of compound **1.** (b) Absorption spectra of the RhB solution during the decomposition reaction under UV irradiation in the presence of compound **2**. (c) Plots of the extent of photodegradation of RhB vs. time (3h) for compounds **1**, **2** and blank. (d) Plots of the extent of photodegradation of RhB vs. time (6h) for compounds **1** and **2.**

Fig. 9 shows the photodegradation results of RhB solutions over various catalysts. As expected, all the catalysts are active for the photodegradation of RhB. About 46.8% (83.2%) of RhB was photodegraded after 3h (6h) using compound **1**. Nevertheless, only about 34.2% (62.9%) of RhB was photodegraded after 3h (6h) using compound **2**.

Compounds **1** and **2** contain the identical metals and the identical organic ligands. In addition, POMs in compounds **1** and **2** are almost identical. The only difference of the POMs of the two is the central atoms. The photocatalytic reaction occurs in an adsorbed phase (on the surface of a catalyst), and the model of activation of a catalyst is photonic activation by exciting a POM with light energy higher than the band gap of the POM, which leads to an intramolecular charge transfer and the formation of a excited-state species (POM*).[26] Therefore, POMs in catalysts are essentially important for their photodegradation properties. We think perhaps the different POMs should be the main reason why compounds **1** and **2** exhibit different conversions.

The second main reason should be perhaps ascribed to the different packing structures of compounds **1-2**. The preferential orientations of crystal planes of compounds **1-2** should be different, thus the number of POMs on crystal planes perhaps should be different too, and the difference perhaps will lead to their different photocatalytic properties. Therefore, the different photocatalytic properties of compounds **1** and **2** can also be due to the different packing structures of the two compounds.

Conclusions

In conclusion, two different 3-D frameworks and two different 2-D frameworks are respectively fused into two novel 3-D POMMOF frameworks. The two novel POMMOF compounds are based on an identical organic ligand. However, the two compounds exhibit distinctly different final structures, the main reason is that the difference of the Keggin species used in the preparations of the two. We just want to further the investigation by using other POMs.

Acknowledgements

This work was supported by National Natural Science Foundation of China under Grant No. 21003056 and 51108122. We thank the help from Dr. De-Chuan Zhao.

Notes and references

[a] *College of Chemistry and State Key Laboratory of Inorganic Synthesis and Preparative Chemistry, Jilin University, Changchun, Jilin, 130023. E-mail:cuixb@mail.jlu.edu.cn.*
[b] *College of Chemistry, Jilin University, Changchun 130023, PR China.*
[c] *Academy of Fundamental and Interdisciplinary Sciences, Harbin Institute of Technology, Harbin, P.R. China, 150080*

† Footnotes should appear here. These might include comments relevant to but not central to the matter under discussion, limited experimental and spectral data, and crystallographic data.

Electronic Supplementary Information (ESI) available: [details of any supplementary information available should be included here]. See DOI: 10.1039/b000000x/

1 (a)D. L. Long, E. Burkholder and L. Cronin, *Chem. Soc. Rev.*, 2007, **36**, 105; (b)M. T. Pope, *Heteropoly and Isopoly Oxometalates*, Springer-Verlag, Berlin, 1983; (c)M. T. Pope and A. Müller, *Angew. Chem., Int. Ed. Engl.*, 1991, **30**, 34; (d)M. T. Pope and A. Müller, *Polyoxometalate Chemistry: From Topology via Self-Assembly to Applications*, the Netherlands, Kluwer, Dordrecht, 2001; (e)T. Yamase and M. T. Pope, *Polyoxometalate Chemistry for Nano-Composite Design*, the Netherlands, Kluwer, Dordrecht, 2002; (f)A. Proust, B. Matt, R. Villanneau, G. Guillemot and G. L. P. Guozerh, *Chem. Soc. Rev.*, 2012, **41**, 7605.
2. A. Müller, P. Kögerler and C. Kuhlmann, *Chem. Commun*, 1999, 1347-1358.
3. C. L. Hill, in *Chem. Rev.*, 1998, vol. 98.
4. (a)J. W. Han and C. L. Hill, *J. Am. Chem. Soc.*, 2007, **129** 15094; (b)R. Cao, J. W. Han, T. M. Anderson, D. A. Hillesheim, K. I. Hardcastle, E. Slonkina, B. Hedman, K. O. Hodgson, M. L. Kirk, D. G. Musaev, K. Morokuma, Y. V. Geletii and C. L. Hill, *Adv. Inorg. Chem.*, 2008, **60** 245.
5. (a)M. I. Khan, E. Yohannes and R. J. Doedens, *Angew. Chem., Int. Ed.*, 1999, **38**, 1292; (b)J. Lu, Y. Xu, N. K. Goh and L. S. Chia, *Chem.*

Commun., 1998, 2733; (c)A. Tripathi, T. Hughbanks and A. Clearfield, *J. Am. Chem. Soc.*, 2003, **125**, 10528; (d)P. J. Hagrman, D. Hagrman and J. Zubieta, *Angew. Chem., Int. Ed.*, 1999, **38**, 2638; (e)S. Reinoso, P. Vitoria, J. M. Gutiérrez-Zorrilla, L. Lezama, L. S. Felices and J. I. Beitia, *Inorg. Chem.*, 2005, **44**, 9731; (f)J. Thomas and A. Ramanan, *Crystal Growth & Design.*, 2008, **8**, 3391.

6. (a)C. Lei, J. G. Mao, Y. Q. Sun and J. L. Song, *Inorg. Chem.*, 2004, **43**, 1964; (b)C. M. Liu, D. Q. Zhang, M. Xiong and D. B. Zhu, *Chem. Commun.*, 2002, 1416; (c)Y. P. Ren, X. J. Kong, X. Y. Hu, M. Sun, L. S. Long, R. B. Huang and L. S. Zheng, *Inorg. Chem.*, 2006, **45**, 4016; (d)G. C. Ou, L. Jiang, X. L. Feng and T. B. Lu, *Dalton Trans.*, 2009, 71; (e)J. Y. Niu, D. J. Guo, J. P. Wang and J. W. Zhao, *Crystal Growth & Design.*, 2004, **4**, 241.
7. (a)X. B. Cui, J. Q. Xu, Y. Li, Y. H. Sun and G. Y. Yang, *Eur. J. Inorg. Chem.*, 2004, 1051; (b)X. B. Cui, J. Q. Xu, H. Meng, S. T. Zheng and G. Y. Yang, *Inorg. Chem.*, 2004, **43**, 8005; (c)C. L. Pan, J. Q. Xu, G. H. Li, X. B. Cui, L. Ye and G. D. Yang, *Dalton Trans.*, 2003, 517; (d)J. W. Zhao, C. M. Wang, J. Zhang, S. T. Zheng and G. Y. Yang, *Chem. Eur. J.*, 2008, **14**, 9223.
8. (a)H. Y. An, Y. G. Li, E. B. Wang, D. R. Xiao, C. Y. Sun and L. Xu, *Inorg. Chem.*, 2005, **44**, 6062; (b)H. Y. An, Y. G. Li, D. R. Xiao, E. B. Wang and C. Y. Sun, *Crystal Growth & Design.*, 2006, **6**, 1107; (c)C. Y. Sun, Y. G. Li, E. B. Wang, D. R. Xiao, H. Y. An and L. Xu, *Inorg. Chem.*, 2007, **46**, 1563; (d)Y. Lu, Y. Xu, E. B. Wang, X. X. Xu and Y. Ma, *Inorg. Chem.*, 2006, **45**, 2060.
9. (a)B. Z. Lin and S. X. Liu, *Chem. Commun.*, 2002, 2126; (b)L. J. Zhang, X. L. Zhao, J. Q. Xu and T. G. Wang, *Dalton Trans.*, 2002, 3275.
10. (a)Y. Wang, L. Ye, T. G. Wang, X. B. Cui, S. Y. Shi, G. W. Wang and J. Q. Xu, *Dalton Trans.*, 2010, **39**, 1916; (b)J. Lü, E. H. Shen, Y. G. Li, D. R. Xiao, E. B. Wang and L. Xu, *Crystal Growth & Design.*, 2005, **5**, 65; (c)J. Q. Sha, J. Peng, H. S. Liu, J. Chen, A. X. Tian and P. P. Zhang, *Inorg. Chem.* , 2007, **46**, 11183; (d)A. X. Tian, J. Ying, J. Peng, J. Q. Sha, H. J. Pang, P. P. Zhang, Y. Chen, M. Zhu and Z. M.Su, *Inorg. Chem.*, 2009, **48**, 100; (e)H. Y. An, E. B. Wang, D. R. Xiao, Y. G. Li, Z. M. Su and L. Xu, *Angew. Chem., Int. Ed.*, 2006, **45**, 904.
11. (a)C. Streb, C. Ritchie, D. L. Long, P. Kögerler and L. Cronin, *Angew. Chem. Int. Ed.*, 2007, **46**, 7579; (b)A. Dolbecq, P. Mialane, L. Lisnard, J. Marrot and F. Sécheresse, *Chem. Eur. J.*, 2003, **9**, 2914; (c)P. Mialane, A. Dolbecq and F. Sécheresse, *Chem. Commun.*, 2006, 3477; (d)B. Nohra, H. E. Moll, L. M. R. Albelo, P. Mialane, J. Marrot, C. Mellot-Draznieks, M. O'Keeffe, R. N. Biboum, J. Lemaire, B. Keita and A. Dolbecq, *J. Am. Chem. Soc.*, 2011, **133**, 13363; (e)S. T. Zheng, J. Zhang and G. Y. Yang, *Angew. Chem. Int. Ed.*, 2008, **47**, 3909.
12. (a) A. Yokoyama, T. Kojima, K. Ohkubo and S. Fukuzumi, *Chem. Commun.*, 2007, 3997; (b) J. P. Wang, J. W. Zhao, X. Y. Duan and J. Y. Niu, *Cryst. Growth Des.,* 2006, **6**, 507; (c) C. M. Liu, D. Q. Zhang and D. B. Zhu, *Cryst. Growth Des.,* 2006, **6**, 524; (d) K. Uehara, H. Nakao, R. Kawamoto, S. Hikichi and N. Mizuno, *Inorg. Chem.,* 2006, **45**, 9448; (e) J. Q. Sha, J. Peng, A. X. Tian, H. S. Liu and J. Chen, *Cryst. Growth Des.,* 2007, **7**, 2535; (f) Y. P. Ren, X. J. Kong, L. S. Long, R. B. Huang and L. S. Zheng, *Cryst. Growth Des.,* 2006, **6**, 572; (g) Y. H. Sun, X. B. Cui, J. Q. Xu, L. Ye, Y. Li and J. Lu, *J. Solid State Chem.,* 2001, **159**, 209; (h) L. L. Fan, D. R. Xiao, E. B. Wang, Y. G. Li, Z. M. Su, X. L. Wang and J. Liu, *Cryst. Growth Des.,* 2007, **7**, 592.
13. (a) H. Abbas, A. L. Pickering, D. L. Long, P. Kögerler and L. Cronin, *Chem. Eur. J.,* 2005, **11**, 1071; (b) C. Streb, C. Ritchie, D. L. Long, P. Kögerler and L. Cronin, *Angew. Chem., Int. Ed. Engl.,* 2007, **46**, 7579; (c) Y. F. Song, H. Abbas, C. Ritchie, N. Mcmillian, D. L. Long, N. Gadegaard and L. Cronin, *J. Mater. Chem.*, 2007, **17**, 1903; (d) T. Mcglone, C. Streb, M. Busquets-Fité, J. Yan, D. Gabb, D. L. Long and L. Cronin, *Cryst. Growth Des.,* 2011, **11**, 2471; (e) E. F. Wilson, H. Abbas, B. J. Duncombe, C. Streb, D. L. Long and L. Cronin, *J. Am. Chem. Soc.,* 2008, **130**, 13876. (f) J. Streb, R. Tsunashima, D. A. Maclaren, T. McGlone, T. Akutagawa, T. Nakamura, A. Scandurra, B. Pignataro, N. Gadegaard and L. Cronin, *Angew. Chem., Int. Ed. Engl.,* 2009, **48**, 6490.
14. (a) Y. P. Xie and C. W. M. Thomas, *J. Am. Chem. Soc.,* 2011, **133**, 3760; (b) G. G. Gao, P. S. Cheng and C. W. M. Thomas, *J. Am. Chem. Soc.,* 2009, **131**, 18257; (c) J. Qiao, K. Shi and Q. M. Wang, *Angew. Chem., Int. Ed. Engl.,* 2010, **49**, 1765; (d) Y. P. Xie and C. W. M. Thomas, *Angew. Chem., Int. Ed. Engl.,* 2012, **51**, 8783.
15. (a) F. Gruber and M. Jansen, *Inorg. Chim. Acta.,* 2010, **363**, 4282; (b) Y. Bai, G. Q. Zhang, D. B. Dang, P. T. Ma, H. Gao and J. Y. Niu, *CrystEngComm*., 2011, **13**, 4181; (c) D. B. Dang, G. S. Zheng, Y. Bai, F. Yang, H. Gao, P. T. Ma and J. Y. Niu, *Inorg. Chem.,* 2011, **50**, 7907.
16. (a) G. Y. Luan, Y. G. Li, S. T. Wang, E. B. Wang, Z. B. Han, C. W. Hu, N. H. Hu and H. Q. Jia, *J. Chem. Soc., Dalton Trans.,* 2003, 233; (b) H. Y. An, Y. G. Li, D. R. Xiao, E. B. Wang and C. Y. Sun, *Cryst. Growth Des.,* 2006, **6**, 1107; (c) H. Y. An, Y. G. Li, E. B. Wang, D. R. Xiao, C. Y. Sun and L. Xu, *Inorg. Chem.,* 2005, **44**, 6062; (d) C. X. Zhang, Y. G. Chen, Q. Tang, Z. C. Zhang, D. D. Liu and H. X. Meng, *Inorg. Chem. Commun.,* 2012, **17**, 155; (e) C. Wang, L. G. Sun, L. L. Lv, L. Ni, S. H. Wang and P. F. Yan, *Inorg. Chem. Commun.,* 2012, **18**, 75; (f) Z. G. Han, Y. L. Zhao, J. Peng, H. Y. Ma, Q. Liu, E. B. Wang, N. H. Hu and H. Q. Jia, *Eur. J. Inorg. Chem.,* 2005, 264; (g)M. Zhu, J. Peng, H. J. Pang, P. P. Zhang, Y. Chen, D. D. Wang, M. G. Liu and Y. H. Wang, *Inorg. Chim. Acta.*, 2010, **363**, 3832; (h) Z. Y. Shi, X. J. Gu, J. Peng and Z. F. Xin, *Eur. J. Inorg. Chem.*, 2005, 3811; (i) X. F. Kuang, X. Y. Wu, J. Zhang and C. Z. Lu, *Chem. Commun.,* 2011, **47**, 3997; (j) B. X. Dong and Q. Xu, *Cryst. Growth Des.,* 2009, **9**, 2776; (k) H. X. Yang, S. Y. Gao, J. Lü, B. Xu, J. X. Lin and R. Cao, *Inorg. Chem.,* 2010, **49**, 736; (l) X. Wang, J. Peng, M. G. Liu, D. D. Wang, C. L. Meng, Y. Li and Z. Y. Shi, *CrystEngComm*., 2012, **14**, 3220; (m) J. X. Chen, T. Y. Lan, Y. B. Huang, C. X. Wei, Z. S. Li and Z. C. Zhang, *J. Solid. State. Chem.,* 2006, **179**, 1904; (n) J. Q. Sha, H. J. Lu, J. Peng, H. J. Pang, A. X. Tian, Y. G. Lv and H. Liu, *Solid. State.Science.,* 2012, **12**, 262; (o) J. Chen, J. Q. Sha, J. Peng, Z. Y. Shi, A. X. Tian and P. P. Zhang, *J. Mol. Struct.,* 2009, **917**, 10; (p) J. Q. Sha, J. Peng, Y. G. Li, P. P. Zhang and H. J. Pang, *Inorg. Chem. Commun.,* 2008, **11**, 907; (q) J. Q. Sha, J. W. Sun, C. Wang, G. M. Li, P. F. Yan and M. T. Li, *Cryst. Growth Des.,* 2012, **12**, 2242; (r) J. Q. Sha, L. Y. Liang, J. W. Sun, A. X. Tian, P. F. Yan, G. M. Li and C. Wang, *Cryst. Growth Des.,* 2012, **12**, 894; (s) Y. Hu, F. Luo and F. F. Dong, *Chem. Commun.,* 2011, **47**, 761.
17. P. Müller, *Crystal Structure Refinement: A Crystallographer's Guide to SHELXL*, Oxford University Press, 2006.
18. I. D. Brown, in Structure and Bonding in Crystals, eds. M. O'Keefe and A. Navrotsky, Academic Press, New York, 1981, ch. 2, pp. 1–30.13.
19. Q. M. Wang, T. C. W. Mak, *Chem. Commun*., 2002, 2682.
20. H. Schmidbaur, W. Bublak, B. Huber, G. Reber, G. Müller, *Angew. Chem. Int. Ed. Engl.*, 1986**, 25**, 1089.
21. E. A. H. Griffith, E. L. Amma, *J. Am. Chem. Soc.*, 1971**, 93**, 3167.
22. A. X. Tian, L. X. Lin, N. Sun, J. Ying, J. W. Zhang, X. L. Wang, *Inorg. Chem. Commun.*, 2014, **40**, 51.

23. (a) T. C. W. Mak, X. L. Zhao, Q. M. Wang, G. C. Guo, *Coor. Chem. Rev.* 2007**, 251**, 2311; (b) M. Munakata, L. P. Wu, G. L. Ning, *Coor. Chem. Rev.* 2000**, 198**, 171.
24. M. X. Liang, C. Z. Ruan, D. Sun, X. J. Kong, Y. P. Ren, L. S. Long, R. B. Huang, L. S. Zheng, *Inorg. Chem*., 2014, **53**, 897.
25. M. G. Liu, P. P. Zhang, J. Peng, H. X. Meng, X. Wang, M. Zhu, D. D. Wang, C. L. Meng and K. Alimaje, *Cryst. Growth Des*., 2012, **12**, 1273.
26. a) H. Fu, Y. G. Li, Y. Lu, W. L. Chen, Q. Wu, J. X. Meng, X. L. Wang, Z. M. Zhang and E. B. Wang, *Cryst. Growth Des.*, 2011, **11**, 458; b) D. Y. Chen, A. Sahasrabudhe, P. Wang, A. Dasgupta, R. X. Yuan, S. Roy, *Dalton Trans.*, 2013, **42**, 10587.

